TOPCon efficiency breakthrough from cell to PV module

Johanna Bonilla, Roman Giehl, Calors Magistris & Roberto Murgioni, JinkoSolar GmbH, Munich, Germany

Abstract

Doped polysilicon-based structures with passivating contacts are expected to rapidly increase their market share, and, along with this, early hopes are starting to materialize for the tunnel oxide passivated contact (TOPCon) cell to be a natural successor to the passivated emitter and rear cell (PERC). Out of other passivated contact technologies, TOPCon is the only one in a similar position to PERC a few years ago when it replaced aluminium back-surface structures (AL-BSF), offering greater efficiency and performance advantages with few additional steps required in production. This paper reviews the steps to making a breakthrough in TOPCon efficiency, from cell to PV module, by using industrially viable manufacturing processes. A detailed characterization and investigation of the primary losses of JinkoSolar's TOPCon record cell of July 2020, with an efficiency of 24.8%, is presented. The results confirmed the high selectivity of the tunnelling oxide and the suppression of the rear-surface recombination by applying a subsequent n^+ poly-Si layer, but also identified that the front-boron-diffused region and resistive losses of the cell accounted for 63% of the electrical losses. These findings allowed further development, and a new record cell efficiency of 25.41% on a 163.75mm × 163.75mm solar cell is reported here, as independently measured in October 2021 by ISFH CalTeC. The transfer of the performance advantages to the module level are also discussed on the basis of laboratory measurements, simulations and complementary real-world field-test results.

Introduction

The market deployment of PV technologies requires a combination of factors be considered in order to achieve success: from a manufacturing perspective, the pressure to achieve higher efficiencies and reliability at competitive costs, while from an investor and developer standpoint, the pursuit for lower levelized cost of electricity (LCOE) to win power purchase agreements (PPAs). This dynamic has prompted extensive research into technological advances. In recent years, p-type passivated emitter and rear contact (PERC) cells have strengthened their market share, reaching 80% at the end of 2021 [1]. As a result of multi-busbar metallization, improvements in wafer quality, selective emitters and other aspects, PERC cells have achieved efficiencies above 24% [2,3]. The transfer of those developments into mass production has assured absolute annual efficiency increases of 0.5–0.6% [4] for PERC cells. Nevertheless, as the efficiency of PERC is reaching its limit, n-type substrates are emerging as the next technological development, moving the solar industry into a new era.

"TOPCon is considered a natural successor to passivated emitter and rear contact (PERC), since it offers technical advantages while only few additional processes are needed."

The expected percentages for the market share of n-type technology differ according to various sources, from 40% in 2031 [1] to an almost complete transition by 2028 [5]. Even for different scenarios, what is clear is that the so-called *n-type passivated contact* cell technologies, which include tunnel oxide passivated contact (TOPCon), interdigitated back contact (IBC) and heterojunction (HJT), have found the right momentum within the solar industry to begin their deployment on a large scale. From a manufacturing perspective, each of these cell architectures follows significantly different process flows. However, of the existing alternatives, TOPCon is considered a natural successor to passivated emitter and rear contact (PERC), since it offers technical advantages (see section 'Performance technical advantages: from cells to modules, from laboratory to real world') while only few additional processes are needed (see section 'Manufacturing process').

Key to the TOPCon cell is the *tunnelling oxide layer*, a structure adopted on the rear side of the n-type wafer. This ultrathin silicon oxide (SiO_x) layer has high selectivity, allowing the majority-charge carriers to *tunnel* through to the subsequent doped polycrystalline silicon layer; the electrons flow at a very low junction resistance, and thus there are negligible losses. At the same time, the tunnelling layer also provides chemical passivation, restraining the minority-carrier recombination.

JinkoSolar's TOPCon development

In terms of efficiency improvement, for PERC cells there is less room. Although the theoretical maximum efficiency is 24.5% [6], factors such as recombination losses, metallization contact regions and carrier transportation performance limit the overall efficiency level that this structure can achieve in a mass production scenario.

Other new alternative contact technologies, such as HJT or IBC, face major challenges with regard to becoming mainstream. HJT makes use of passivated contacts based on a layer stack of intrinsic and doped amorphous silicon, which implies a parasitic absorption in the front layer stack and consequently a reduction in short-circuit current. Its manufacture involves higher production tool costs, since processes above 200°C cannot be used after the amorphous silicon deposition. Moreover, there is a growing need to reduce the amount of silver, or replace it with copper, as well as cut down the use of indium in the transparent conductive oxide (TCO) layer [6]. IBC, on the other hand, needs to meet the challenge of becoming cost-competitive, because of the production complexity for obtaining perfectly fine and aligned layers, since it has doping and contacts of both polarities on one side.

On the production side, TOPCon offers a natural extension of PERC lines – with a few steps added – while providing improved efficiency and plenty of room for further improvement. With the highest theoretical efficiency of 28.75%, TOPCon is already close to the maximum theoretical conversion efficiency achievable by monocrystalline silicon cells [7,8].

The maximum cell efficiency increases linearly with the selectivity S_{10}, until the radiative recombination starts to limit further growth. This behaviour justifies the logarithmically scaled selectivity, defined as $S_{10} = \log_{10}[V_{th}/(J_o{}^*\rho_c)]$, as shown in Fig. 1(b). It therefore depends on the thermal voltage V_{th}, the recombination current density J_o and the contact resistance ρ_c.

JinkoSolar's TOPCon high selectivity relies on applying to the rear side of the n-type wafer a stack of silicon oxide and doped polysilicon films, providing a highly asymmetric equilibrium carrier concentration of majority and minority carriers in the contact, as detailed in Fig. 1(c).

Manufacturing process

JinkoSolar TOPCon wafers are prepared from Czochralski-grown (Cz) phosphorus-doped n-type monocrystalline silicon, with resistivity in the range 0.3–2.1Ω·cm and of size 182mm × 182mm, cut from a diameter of 253mm. Fig. 2, outlines the cell fabrication process.

Texturing

The process starts with texturing of the n type silicon wafers. The wafers are placed in a commercial alkaline solution (KOH) containing organic additives to form pyramid structures. This step serves to reduce reflection.

Boron diffusion

The wafers are then placed into a boron diffusion tube furnace (BCl_3 as a source) to form a homogeneous p^+-doped emitter layer.

Etching

The rear p^+-doped region is removed using an industrial alkaline single-side etching process to form the optimized rear-surface morphology.

Tunnelling oxide and poly-Si

Low-pressure chemical vapour deposition (LPCVD) at 500–600°C allows the in situ thermal oxidation of the crystalline silicon (c-Si) surface to form an ultrathin tunnelling oxide (SiO_x) before the poly-Si growth. The n^+ doping of the intrinsic poly-Si is carried out in a $POCl_3$ diffusion furnace and the

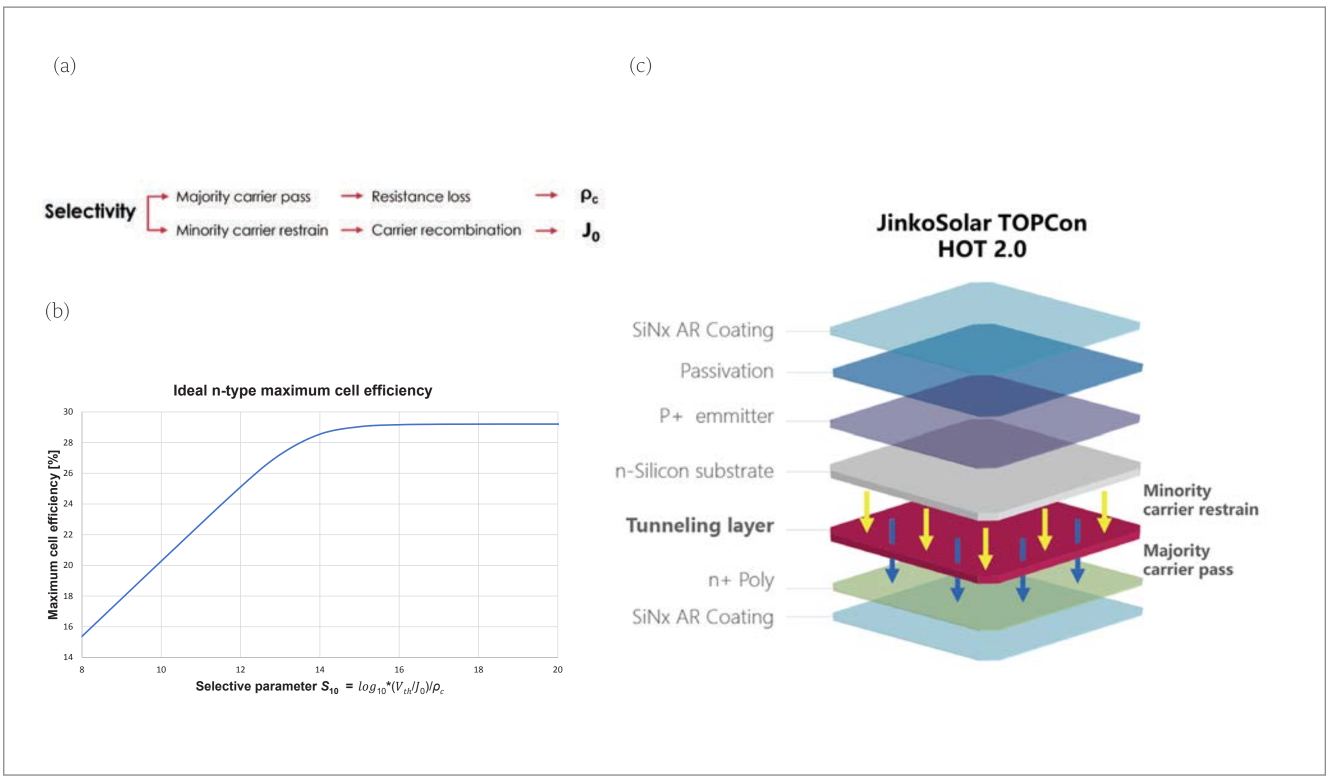

Figure 1. (a) Influence of passivation on majority and minority carriers. (b) Theoretical maximum efficiency as a function of the S_{10} selectivity of an n-type cell from a 2Ω·cm wafer of thickness W = 110µm, with Lambertian light trapping (J_{sc} =43.6mA/cm^2) and with a single contact of selectivity S_{10}. The other contact is ideal, as described in Brendel et al. [7]. (c) JinkoSolar TOPCon structure, showing in red the tunnelling oxide layer.

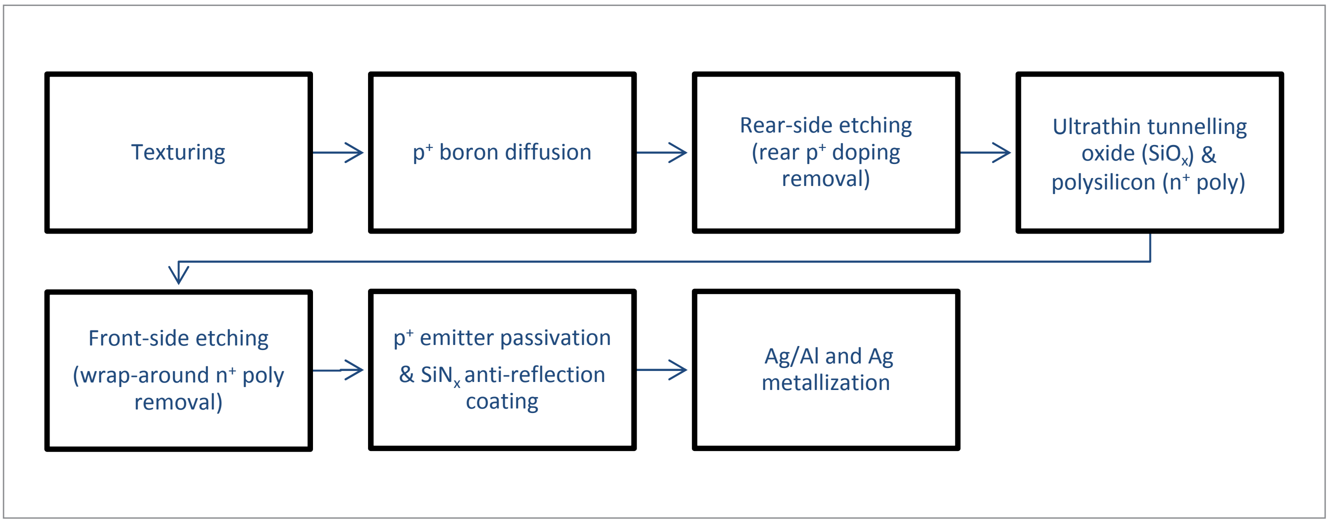

Figure 2. TOPCon cell manufacturing process.

n+ poly-Si is formed. The n+ poly-Si layer is less than 150nm in thickness, with a uniform doping profile within the poly-Si layer of about $3 \times 10^{20} cm^{-3}$, as measured using electrochemical capacitance–voltage (ECV).

It is important to mention that other methods can be used for the deposition of passivated contact cells, such as plasma-enhanced chemical vapour deposition (PECVD) and atmospheric pressure chemical vapour deposition (APCVD). However, LPCVD is a mature process, as it has been extensively used in the semiconductor industry for the deposition of poly-Si. In LPCVD, thin films are deposited from gas-phase precursors in a vacuum. In the course of this thermal process, the reduced pressure helps to prevent undesirable gas-phase reactions and to improve the field uniformity on the wafer. During the poly-Si deposition, silane gas is used as the reaction source, which is injected into the LPCVD tube and pyrolyses around the quartz wafer carriers. Suitable optimization of the process can provide a consistent reaction environment in terms of wafer temperature and nearby reactive gas flow; this results in excellent uniformity of the thin-film thickness and quality across the whole tube, as seen in Fig. 3.

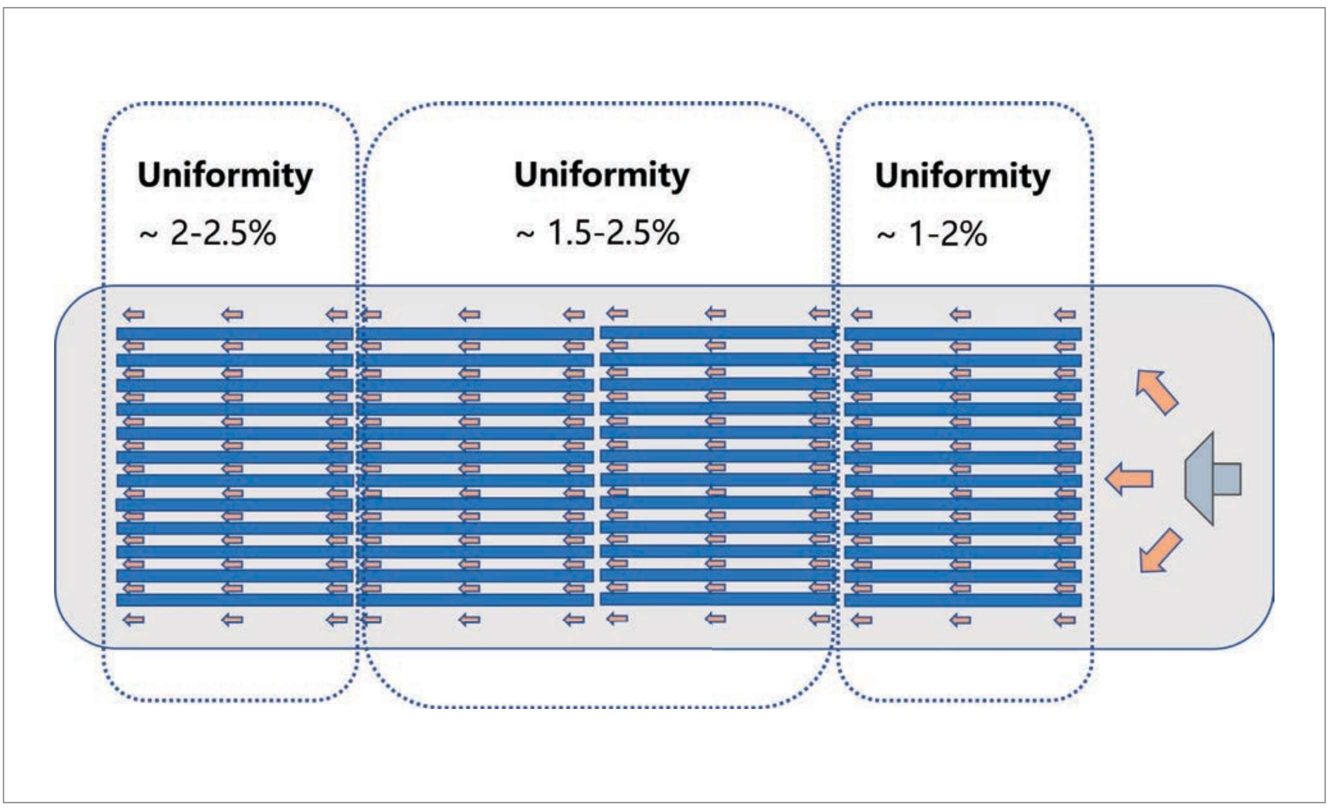

Figure 3. Uniformity of thin-film thickness and quality across the low-pressure chemical vapour deposition LPCVD tube. During the poly-Si deposition process, silane gas is used as the reaction source, which is injected into the LPCVD tube and pyrolyses around the quartz wafer carriers.

The challenges of LPCVD lie in being able to control the undesirable deposition of the poly-Si layer on the front, known as *wrap-around*. JinkoSolar's experience in the production of n-type technology, however, has enabled significant improvements to be made to the LPCVD configuration, resulting in a tweaked horizontal-loading LPCVD; moreover, an active wrap-around removal process (next process step) has been implemented, which assures the wrap-around is kept within acceptable limits, reducing the negative impact on the yield.

Removal (front-side etching)

Since the poly-Si is inherently deposited on both sides of the wafer, a wrap-around etching process is performed using a feasible mass-production chemical wet bench. With appropriate process control, the front-side p^+ emitter can be well protected, as shown in Fig. 4. The front-side borosilicate glass (BSG) and the rear-side phosphosilicate glass (PSG) layers are removed in diluted HF solution, followed by a cleaning stage.

p^+ emitter passivation and SiN_x anti-reflection coating

This step involves the passivation of the p^+ emitter side and the SiN_x anti-reflection (AR) coating, and the AR coating of the n^+ poly side.

Ag and Al metallization

Ag/Al and Ag pastes are screen printed and then co-fired in a belt furnace to form the front and rear contact grids, respectively.

Investigation of primary losses and pathways for further TOPCon efficiency improvement

Many players in the solar industry are competing in a perpetual race to achieve high efficiencies. To this end, JinkoSolar has been undertaking a long path of research and development of n-type cell structures since 2017, establishing various world records at the cell and module levels, as detailed in Fig. 5. In support of that work, the goal was the definition and implementation of viable industrial manufacturing processes for performance improvements.

In July 2020 JinkoSolar's record cell, with an efficiency η of 24.79% on a 163.75mm × 163.75mm solar cell, was reported and independently measured by ISFH CalTeC. This cell was characterized in detail and further simulations were performed in order to investigate the primary power and energy losses [9]. The results showed that rear-surface recombination is effectively suppressed by applying n^+ poly-Si, but 63% of the electrical losses can be attributed to the front-boron-diffused region and resistive losses of the cell.

Record cell recombination parameter results

The recombination current (J_o) values of the passivated and metallized fractions of the front layer of the rear surface were determined by using high-resistivity 10Ω·cm n-type wafers. Double-

“An active wrap-around removal process has been implemented, which assures the wrap-around is kept within acceptable limits, reducing the negative impact on the yield.”

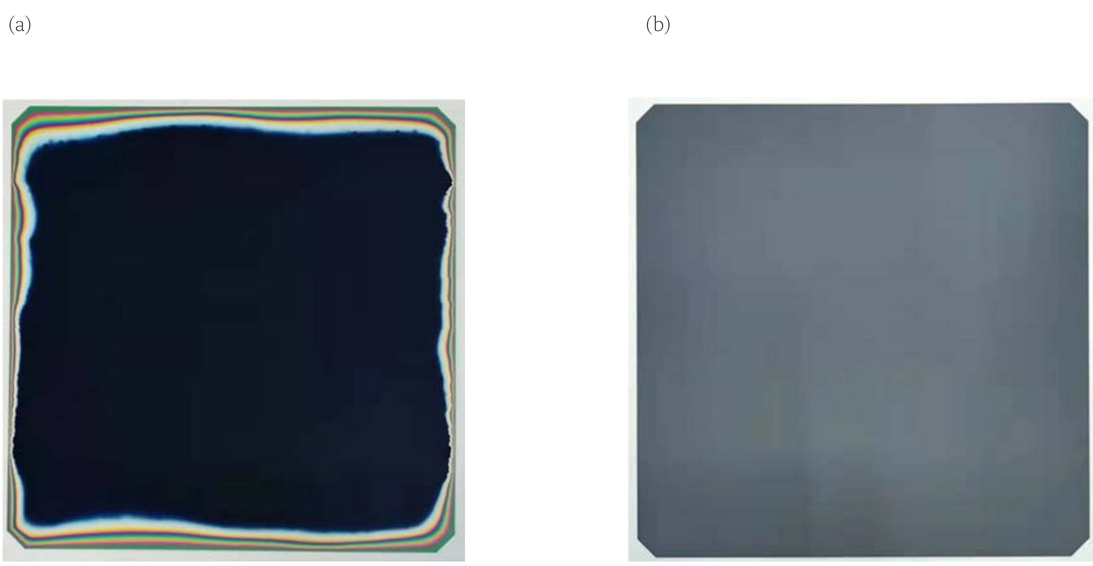

Figure 4. (a) Wafer before the wrap-around removal. (b) Wafer after wrap-around poly-Si layer removal using JinkoSolar etching technology.

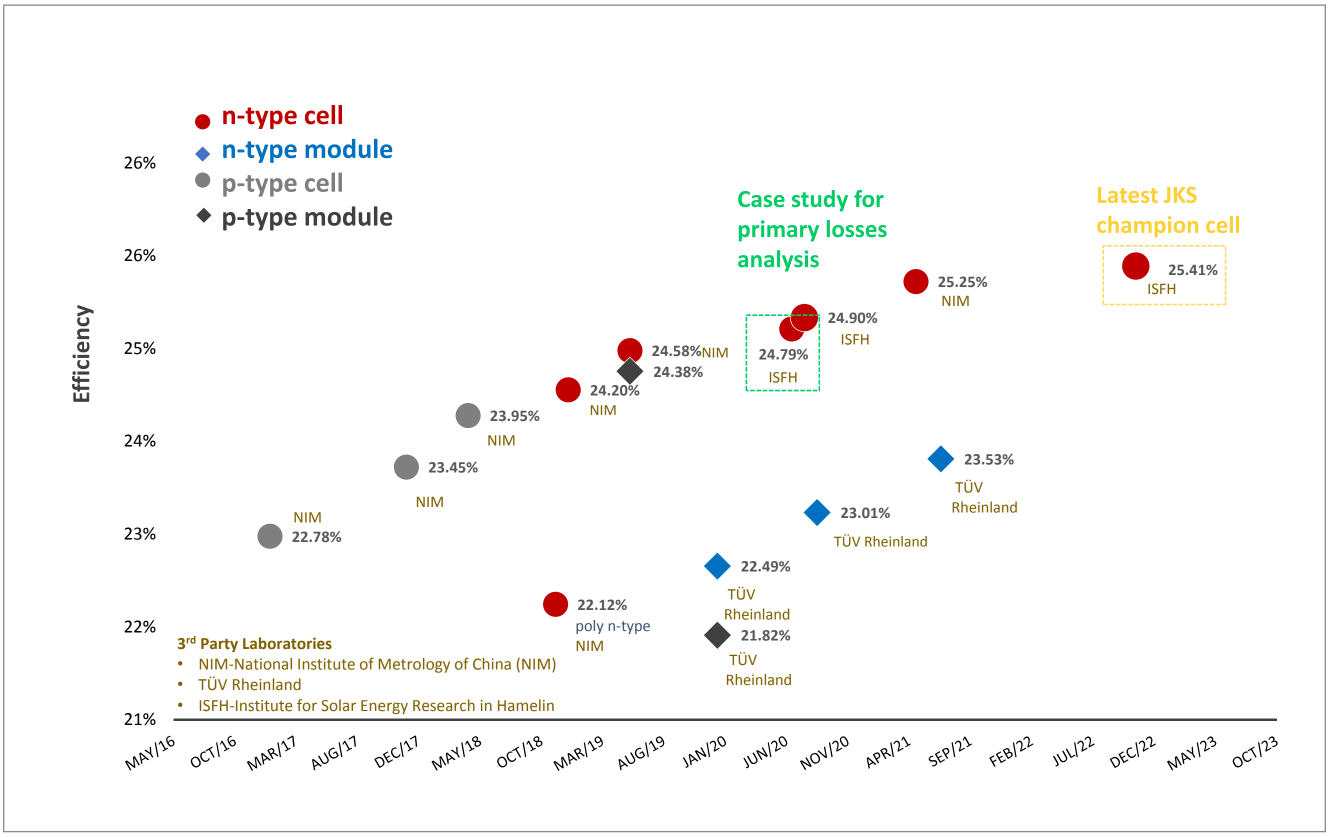

Figure 5. JinkoSolar world efficiency records: marked in green is the cell used for the primary loss case study, and in yellow, the latest champion cell. Both efficiency measurements were performed independently by ISFH CalTeC under standard test conditions.

side boron-diffused textured wafers were used for the front-side J_o measurement. To analyse the effect of additional thermal budget on the boron doping and associated changes in recombination, the wafers were masked and subjected to $POCl_3$ diffusion. Multiple thin-film stacks (Al_2O_3/SiN_x) were used for passivation, followed by firing of the samples in the same belt furnace as the cells. The excellent quality of the front-side passivation was demonstrated by the value obtained for $J_{o,front}$ of 6.2fA/cm² [9].

For the rear n⁺ poly-Si structure, wafers were etched in the same industrial HF/HNO_3 solution as the cells, and subsequently passivated with PECVD SiN_x and fired along with the cells; the resulting value of $J_{o,rear}$ was 3.2fA/cm². The study also assessed the J_o of the front Ag/Al-contacted area, by using double-side boron-diffused textured wafers and applying different metallization fractions (0% to 37%) to the rear side; the value of J_o was found to be 720fA/cm².

Although the J_o between the Ag paste and the n⁺ poly-Si region for the rear side was not accurately determined, the upper limit was established to be 50fA/cm² in the study [9].

Record cell series resistance

The resistance of the Ag/Al paste was 2.2mΩ·cm² for the front side and 1.0mΩ·cm² for the rear. The latter was an estimation of the contact resistivity between the Ag and the poly-Si, since no removal of the poly-Si was performed. Therefore, the series resistance R_s was determined by comparing the Suns-V_{oc} method with the light I–V measurement at the maximum power point. The resulting pseudo-fill factor (pFF) of the record cell was 84.96%, and the effective R_s of the cell was determined to be 0.2Ω·cm².

Record cell simulation

Additional simulations were carried out to identify avenues to explore for further improvement of the state-of the-art manufacturing processes. A three-dimensional simulation based on the reported measured recombination and resistance values was used to analyse optical losses.

Optical losses

The external quantum efficiency (EQE) of the TOPCon record cell showed a superior blue response (wavelength range 300–500nm) as a result of the optimization of both the boron-diffused region and the anti-reflection coating (ARC). Front-grid shading (1.2mA/cm²), escape reflection (1.4mA/cm²) and bulk and rear parasitic infrared absorption (1.8mA/cm²) contributed to the major optical losses, as illustrated in Fig. 6(a).

On the basis of these results, it is possible to identify lines of approach for achieving optical improvements. Front-grid shading losses, for example, can be limited by reducing the finger width and contact resistivity. Developments in

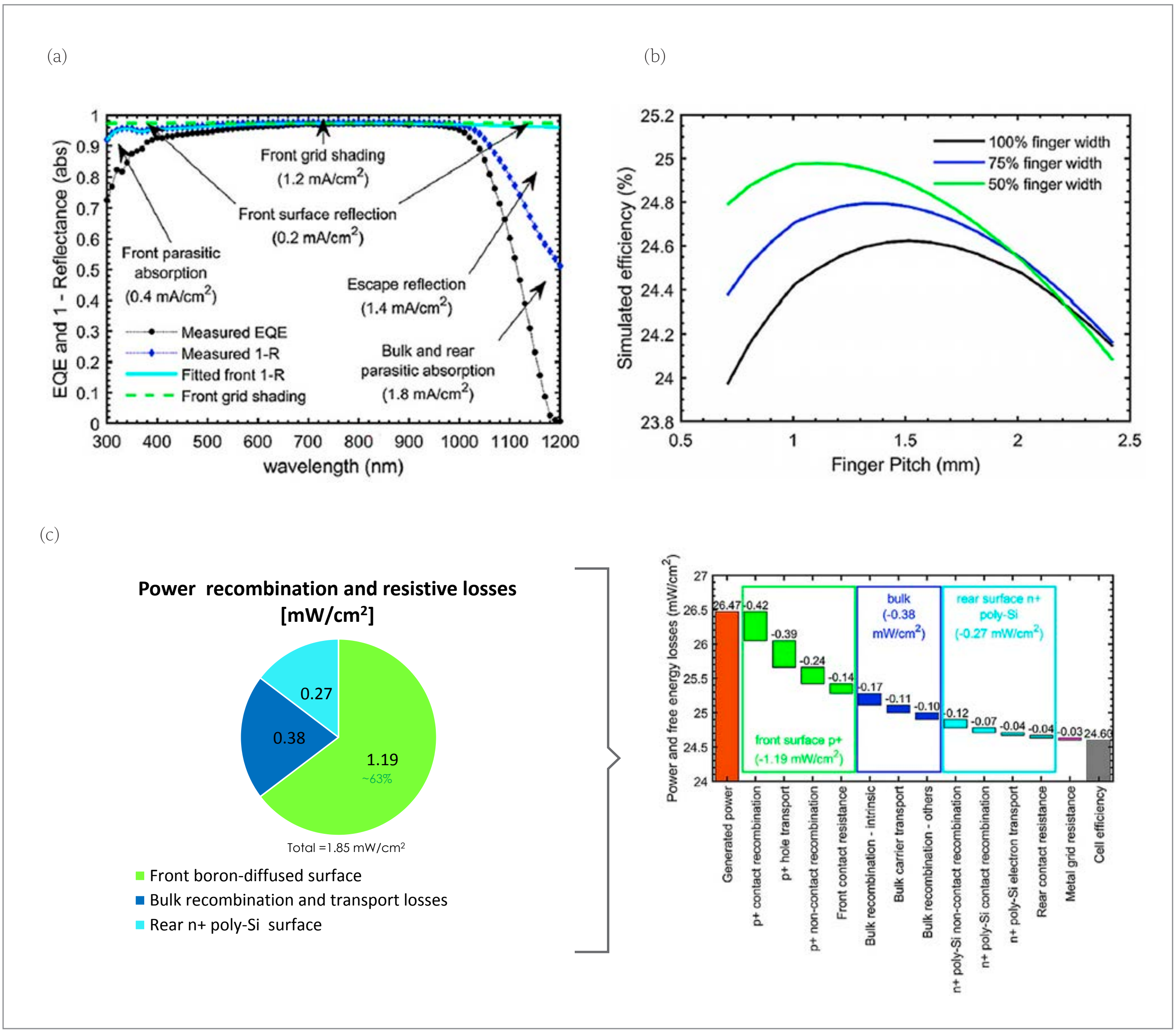

Figure 6. Analysis of the losses of the record cell with η = 24.8% [9]. (a) Optical analysis losses, showing the measured EQE (performed independently by ISFH CalTeC). (b) Results of cell efficiency simulations as a function of the front-finger pitch for 100%, 75% and 50% finger widths. (c) FELA results, based on simulations. The total recombination and resistive losses are 1.85mW/cm^2.

gridding are ongoing and expectations are high; according to ITRPV [1], finger widths from 36 to 20µm are expected by 2031. In addition, narrower fingers also allow smaller pitch, improving the performance of the boron emitter of the front side. The simulations results, as shown in Fig. 6(b), demonstrated that a reduction of 25% in the finger width improved the efficiency by 0.2%$_{abs}$, and a further reduction of 50% resulted in an additional 0.2%$_{abs}$ efficiency improvement [9].

Electrical losses

The free energy loss analysis method (FELA), as described in Brendel et al. [7], was used for the electrical analysis. Fig. 6(c) shows the breakdown of the power losses, which amounted to 1.85mW/cm^2 overall. The boron-diffused region on the front surface accounted for losses of 1.19mW/cm^2, representing 63% of the total losses. Out of this, the single largest contributor was the p^+ contact recombination, with 0.42mW/cm^2. Reported bulk recombination and transport losses were 0.38mW/cm^2, while the rear-side n^+ poly-Si accounted for total minor losses of 0.27mW/cm^2 [9]. In the same way, pathways for further improvement for the optimization of the boron-diffused front surface were revealed, in agreement with Chen et al. [10].

Implementation of findings: boosting large-area efficiency to 25.41%

The findings of the detailed analysis in 2021 were used to advantage to enable further cell developments, allowing JinkoSolar to establish a new cell efficiency record of 25.41% on a large-area TOPCon cell by the end of that year. The main current–voltage (*I–V*) parameters are detailed in Table 1, and the independent measurement by ISFH CalTeC is shown in Fig. 7.

Cell I–V parameter	Measured result
V_{oc} [mV]	719.1
J_{sc} [mA/cm^2]	42.24
FF [%]	83.66
η [%]	25.41

Table 1. Measured current–voltage (*I–V*) parameters of JinkoSolar's latest large-area n-type TOPCon record cell.

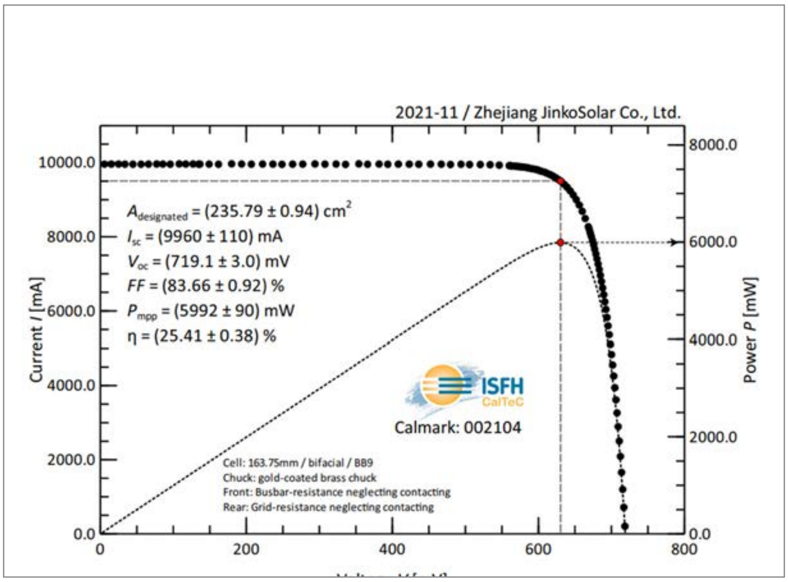

Figure 7. Illuminated current–voltage and power–voltage characteristics of JinkoSolar's latest large-area n-type TOPCon record cell, with 25.41%. The measurement was independently performed by ISFH CalTeC under standard test conditions.

"The TOPCon cell has a natural immunity to boron–oxygen-related LID, and well as resistance to LeTID."

Specific key factors for improving cell efficiency were:

1. The morphology of the rear-side surface was optimized and the poly-Si layer thickness was reduced, to enhance the spectral response of the cell in the infrared range, resulting in increased short-circuit current.

2. Surface passivation quality was enhanced on both front and rear cell surfaces, as a result of systematic process optimization of the passivation layer, as well as the tunnelling oxide/poly-Si stack.

3. The cell structure at the front was optimized, resulting in improved passivation quality and spectral response in both UV and visible light ranges. Thus, impressive values of V_{oc} and J_{sc} were achieved.

Performance technical advantages: from cells to modules, from laboratory to real world

TOPCon's response to LID/LeTID

Because of its structural make-up, the TOPCon cell has a natural immunity to boron–oxygen-related light-induced degradation (LID), as well as resistance to light- and elevated-temperature-induced degradation (LeTID). The higher tolerance to impurities means that these advantages can be seen not only in the laboratory but also in mass production. Although the nature of the LeTID effect has been extensively investigated, the hypotheses proposed for its constitution are diverse. Several studies attribute the degradation effect to metallic impurities [11–14]; however, more current evidence points to the participation of hydrogen in this phenomenon [15,16].

It has been found that the hydrogenated silicon nitride (SiN_x:H) film is able to release hydrogen into the silicon bulk during fast firing [17–19]. Jensen et al. [20], however, demonstrated the presence of LeTID with plasma hydrogenation as well, linking the phenomenon to hydrogen and not to the technique.

With the discussion still open regarding the cause, what has become clear from these studies is that n-type modules are less sensitive to this phenomenon, which implies a reduction in losses. Jinko has also verified this by independent laboratory tests, and it is an attractive factor for long-term investments.

Power–temperature coefficient (γ)

The temperature-dependent rate of change of each I–V parameter – namely the maximum output power (P_{max}), the short-circuit current (I_{sc}) and the open-circuit voltage (V_{oc}) – can be described through the so-called *temperature coefficients*. To determine these coefficients, a sweep of I–V curves is performed under different temperatures and a constant illumination of 1,000W/m^2. The slope of the least-squares-fit straight line of the plotted I–V parameter as a function of temperature determines its respective coefficient [21].

The factor that most decisively characterizes energy efficiency losses due to temperature during operation is the P_{max} temperature coefficient, designated by γ. It is inversely proportional to the temperature change (–%/K); therefore, to obtain high yields, the value of γ should be as low as possible. Power–temperature coefficients depend more on cell technology than on manufacturing processes or PV module design. Here, JinkoSolar TOPCon structures, with –0.30%/°C, offer a natural advantage over PERC, with 0.35%/°C, and even over other n-type cell technologies, such as passivated emitter, rear totally diffused (PERT), with 0.32%/°C (see Fig. 8).

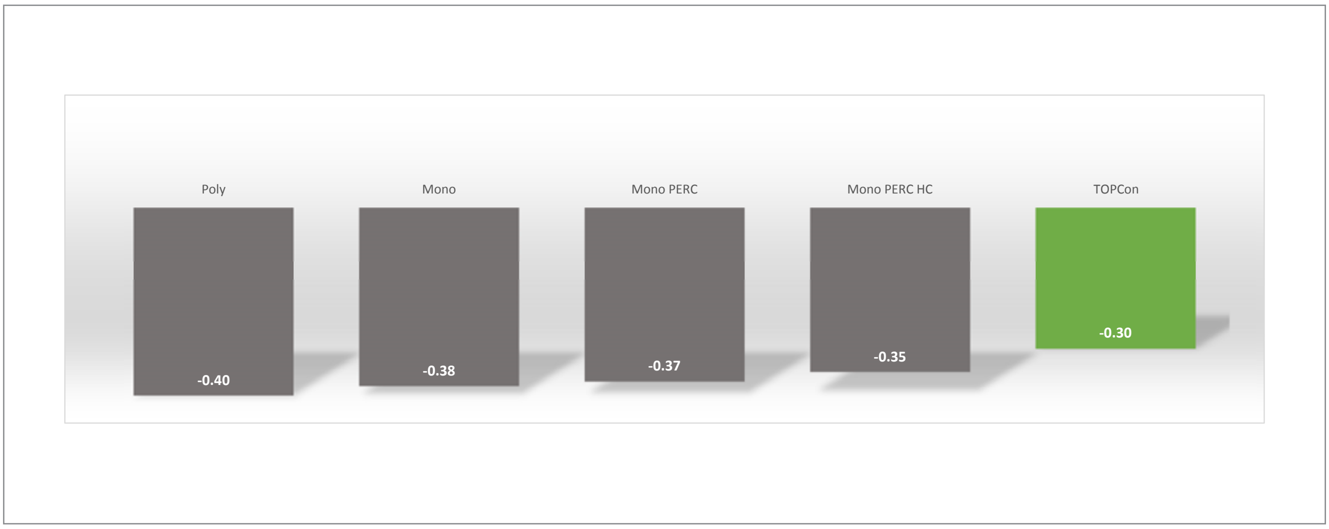

Figure 8. Power–temperature coefficient (γ) for different cell technologies. Values have improved with every generation of PV technology, but the switch from PERC to TOPCon will further improve it by +15%.

Bifaciality

Bifaciality is the efficiency ratio between the rear side and the front side under standard conditions, specified as an irradiance of 1,000W/m^2, a temperature of 25°C and an air mass of 1.5 [22]. An advantage of TOPCon structures over PERC technologies is their higher bifaciality, which is ~85% at the cell level. Fig. 9 shows the bifaciality results for a 182mm production cell.

A higher bifaciality means a higher utilization of the irradiance on the rear side of the module, which in turn means an increase in energy. At the module level, the bifaciality of n-type modules is ~80%, compared with ~70% for most p-type modules. The increase in production, in turn, results in a reduction in the LCOE. The degree of importance of this factor will be determined by the specific project, and depends on the reflectivity (albedo) and installation conditions. However, when all these factors are kept constant, and only the bifaciality is varied, an overall advantage is seen.

Table 2 shows the simulation results for a 3MW PV power plant in Syców, Poland. The same module was used to obtain the system production when just the bifaciality factor was varied, with the rest of the installation and environmental conditions kept constant. The results show an energy contribution of up to 1.5% by changing the bifaciality factor, in addition to a bifacial gain of 7.4%.

From a manufacturing point of view, improving bifaciality is a complex trade-off task. On the one hand, enhancing the front side of the cells, while representing an overall improvement, also implies a negative impact of the bifaciality; on the other hand, only improving the bifaciality does not fully contribute to an upgrade. Therefore, resources are allocated, as a first step, to an improvement of the front side as a priority, and, in a second step, to the improvement of the bifaciality. Improving the latter feature of the structure can be done

> "To obtain high yields, the value of the P_{max} temperature coefficient γ should be as low as possible."

either by changing the wafer thickness, which will directly reduce the light absorption in the doped polysilicon layer, or by improving other aspects, such as the wafer passivation and quality, the metallization through reducing rear-side shading, and the rear-side structure through texturing or polishing.

Low irradiance performance

Fig. 10 shows a comparison of the low-irradiance behaviour for n-type and p-type modules. The *I–V* performance at different irradiances was measured with a pulsed solar simulator, varying

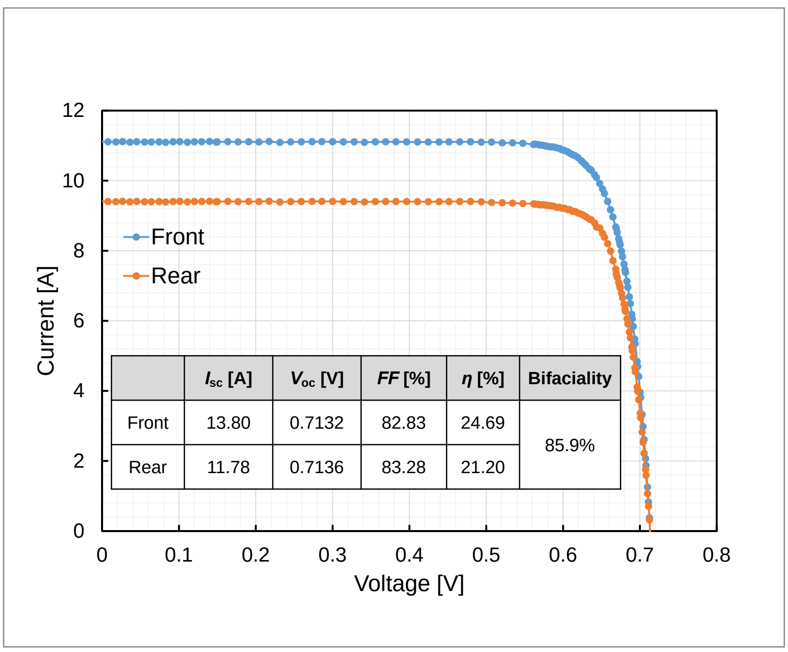

	I_{sc} [A]	V_{oc} [V]	*FF* [%]	η [%]	Bifaciality
Front	13.80	0.7132	82.83	24.69	85.9%
Rear	11.78	0.7136	83.28	21.20	

Figure 9. *I–V* characteristics of the front and rear sides for a 182mm production cell.

Location	Syców, Poland (51.31°N, 17.72°E)			
Capacity	3MW (front only)			
Albedo	25–30%			
Height	1.5			
Tilt	30°			
Module	Bifaciality factor	System production [MWh/a]	Bifacial gain [%]	ΔGain [%]
Monofacial n-type 550W	0	3340	Monofacial	Benchmark
Bifacial n-type 550W	0.70	3587	7.40	7.40
Bifacial n-type 550W	0.75	3605	7.90	0.50
Bifacial n-type 550W	0.80	3622	8.37	0.98
Bifacial n-type 550W	0.85	3640	8.87	1.48

**Module Tiger Neo Bifacial JKM550N-72HL4-BDV*

Table 2. PVSyst simulation results for a 3MW PV plant in Poland, with variations of only the bifaciality factor, with all other module, ambient and installation conditions remaining the same.

the irradiance from G = 100W/m² up to G = 1,000W/m², in accordance with the IEC 61853-1 standard [23]. The homogeneity of the irradiance was tracked in order to satisfy the requirements of IEC 60904-9 [24]. The relative efficiency was calculated to be:

$$\eta_{rel} = \frac{P_{max,meas} \cdot 1{,}000\,W/m^2}{G_{meas} \cdot P_{max,STC}} \quad (1)$$

The performance at low irradiance depends more on the manufacturing processes and PV module design than on the cell technology itself [25,26]. At the module level, n-type technologies achieve high parallel resistance to reduce losses at low illumination, while low series resistance reduces the losses at high currents.

Performance of n-type PV modules under real-world conditions

TOPCon's higher efficiencies at the cell level are

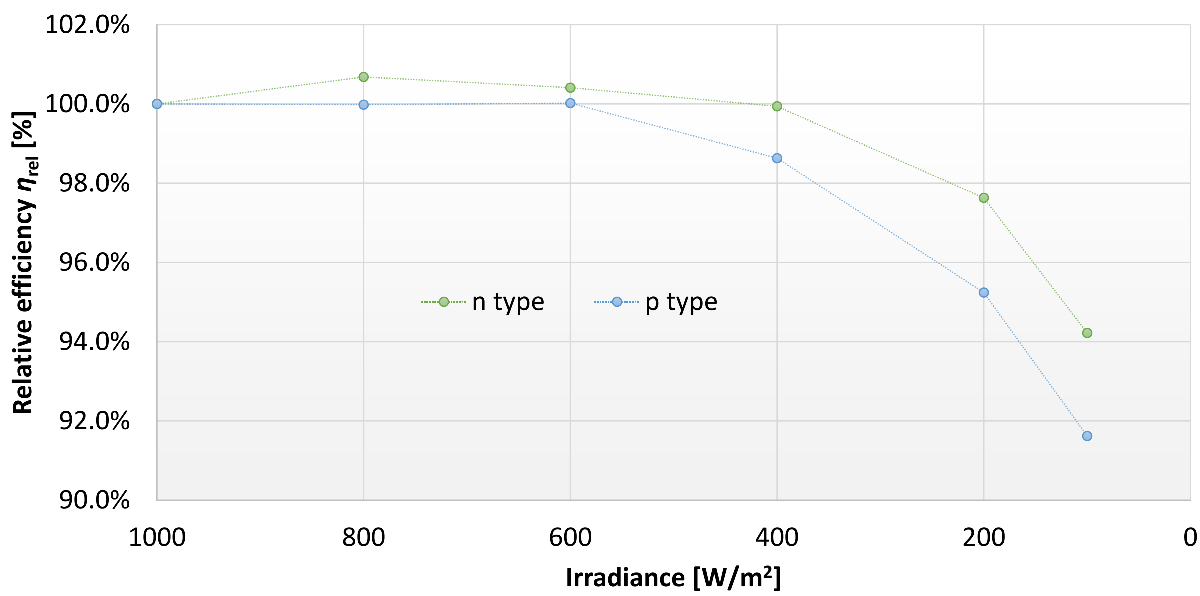

Figure 10. Low-irradiance performance of n-type and p-type modules. *I–V* measurements were taken in a pulsed solar simulator at irradiances G ranging from 100W/m² to 1,000W/m², in accordance with IEC 61853-1.

reflected in enhanced performance at the module level and have already been verified by outdoor test results. JinkoSolar has compiled a series of field results since 2019 for 163mm wafer modules in different locations around the world.

At the NWS location, in Australia, the performance of bifacial modules was monitored from December 2019 until May 2020, in order to contrast with their monofacial equivalents. Three types of module were deployed: one monofacial (p-type), along with one bifacial n-type and one bifacial p-type, both with a transparent backsheet. The bifacial gain for the n-type module averaged 10.86% and for the p-type, 7.80%, which represents an increase of 3.06% due to cell technology alone, as shown in Fig. 11(a).

At the Ningxia location, in China, two strings incorporating bifacial n-type and p-type tilling ribbon (TR) technology, both with a transparent backsheet, were compared. The results revealed an increase in energy generation of 2.7% for n-type over p-type, as shown in Fig. 11(b).

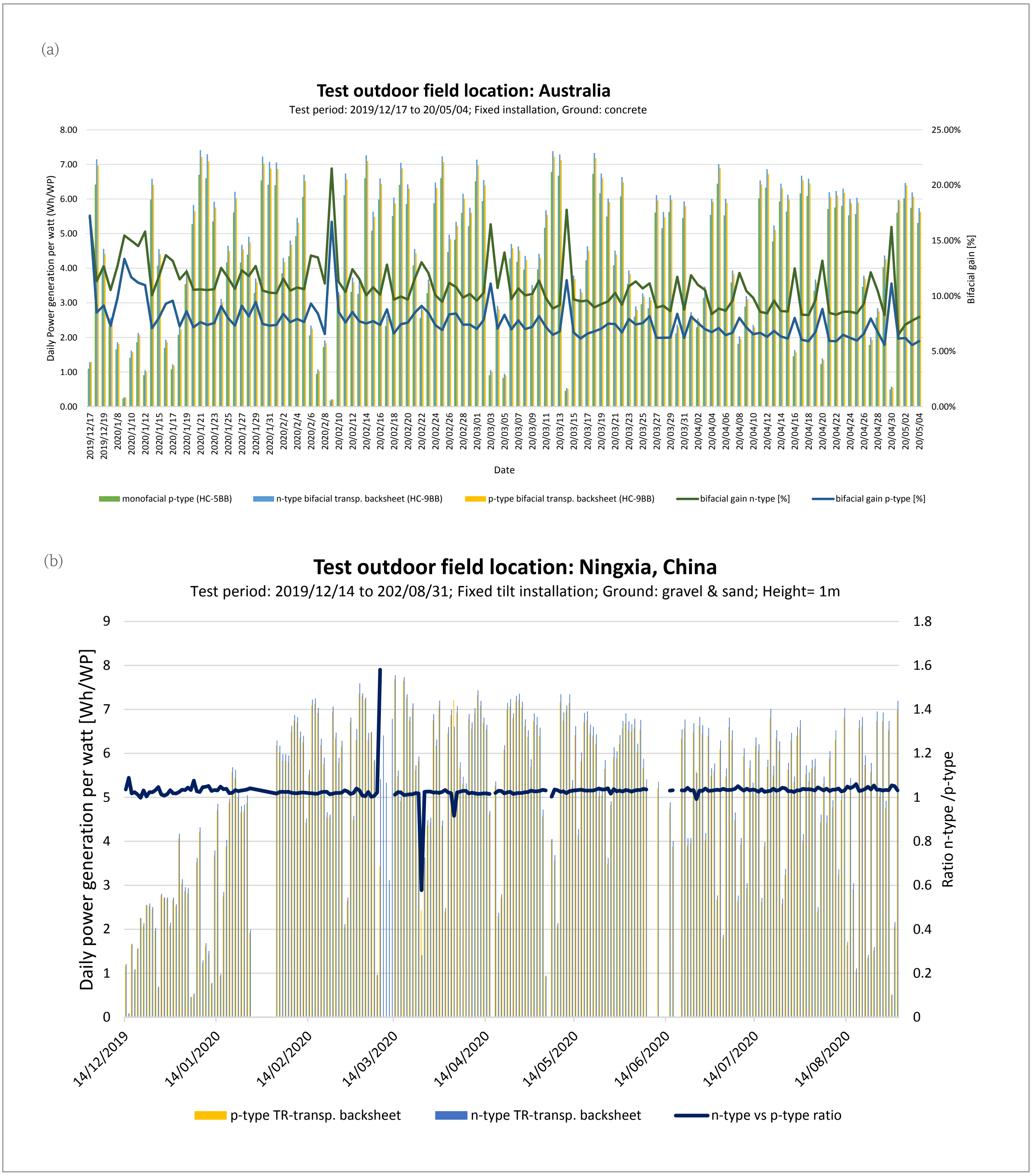

Figure 11. Results of outdoor tests for different locations: (a) Australia, with daily resolution. (b) Ningxia, China, with daily resolution.

"Further efforts will focus on achieving TOPCon's theoretical limit, based on large wafer sizes, with economically feasible procedures for mass production."

These results have been reproduced at different locations, where the energy production advantages of n-type modules have ranged from 1.5 to 3% compared with p-type modules.

Summary and conclusions

Several factors are responsible for establishing n-type TOPCon cell technologies in a key leading position for the next PV technology transition:

- Technological and economic limits are being reached with regard to efficiency improvements of PERC structures (currently about 24%), with little room remaining for further viable production improvements.
- Project developers are demanding better efficiencies at increasingly competitive costs.
- TOPCon's similarities in production to its PERC equivalent offer advantages over other doped polysilicon-based passivating-contact structures, not only in manufacturability but also in performance, with the highest theoretical maximum efficiency within these structures.

This paper has presented JinkoSolar's efforts in researching this particular cell structure, which has led to the launch of large-scale production of TOPCon modules. As an example, the power loss analysis of the 2020 best-performing cell with a record 24.8% was presented, and on the basis of these results, the implemented improvements that led to a new record of 25.4% by the end of 2021 were discussed. Both efficiencies were independently measured by ISFH CalTeC on a 163.75mm × 163.75mm solar cell.

Given that the advantages of the TOPCon cell are also reflected at the module level, and have been verified at JinkoSolar's outdoor test centres, further efforts will focus on achieving TOPCon's theoretical limit, based on large wafer sizes, with economically feasible procedures for mass production.

Acknowledgements

The authors would like to thank P. Zheng and the rest of our colleagues at Jinko Solar in China, as well as the Australian National University for the supporting data.

References

[1] VDMA 2021, "International technology roadmap for photovoltaic (ITRPV): 2020 results", 12th edn (Nov.) [https://itrpv.vdma.org/en/].
[2] Green, M. et al. 2021, "Solar cell efficiency tables (version 57)", *Prog. Photovolt: Res. Appl.,* Vol. 29, No. 1, pp. 3–15, doi:10.1002/pip.3371.
[3] Min, B. et al. 2017, "A roadmap toward 24% efficient PERC solar cells in industrial mass production", *IEEE J. Photovolt.,* Vol. 7, No. 6, pp. 1541–1550, doi:10.1109/JPHOTOV.2017.2749007.
[4] Hermle, M. et al. 2019, "Passivating contacts and tandem concepts: Approaches for the highest silicon-based solar cell efficiencies", *AIP Appl. Phys. Rev.,* doi:10.1063/1.5139202.
[5] PV Tech Research 2021, "PV manufacturing & technology quarterly report" (May release).
[6] Wilson, G. et al. 2020, "The 2020 photovoltaic technologies roadmap", *J. Phys. D: Appl. Phys.,* Vol. 53, doi:10.1088/1361-6463/ab9c6a.
[7] Brendel, R., Rienaecker, M. & Peibst, R. 2016, "A quantitative measure for the carrier selectivity of contacts to solar cells", *Proc. 32nd EU PVSEC*, Munich, Germany, doi:10.4229/EUPVSEC20162016-2CO.4.1.
[8] Brendel, R. & Peibst, R. 2016, "Contact selectivity and efficiency in crystalline silicon photovoltaics", *IEEE J. Photovolt.*, Vol. 6, No. 6, pp. 1413–1420, doi:10.1109/JPHOTOV.2016.2598267.
[9] Zheng, P. et al. 2021, "Detailed loss analysis of 24.8% large-area screen-printed n-type solar cell with polysilicon passivating contact", *Cell Rep. Phys. Sci.,* Vol. 2, No. 10, doi:10.1016/j.xcrp.2021.100603.
[10] Chen, D. et al. 2020, "24.58% total area efficiency of screen-printed, large area industrial silicon solar cells with the tunnel oxide passivated contacts (i-TOPCon) design", *Sol. Energy Mater. Sol. Cells,* Vol. 206, p. 110258, doi:10.1016/j.solmat.2019.110258.
[11] Jensen, M.A. et al. 2018, "Solubility and diffusivity: Important metrics in the search for the root cause of light- and elevated temperature-induced degradation", *IEEE J. Photovolt.,* Vol. 8, No. 2, pp. 448–455, doi:10.1109/JPHOTOV.2018.2791411.
[12] Wagner, M. et al. 2018, "Correlation of the LeTID amplitude to the aluminium bulk concentration and oxygen precipitation in PERC solar cells", *Sol. Energy Mater. Sol. Cells,* Vol. 187, pp. 176–188, doi:10.1016/j.solmat.2018.06.009.
[13] Morishige, A.E. et al. 2016, "Lifetime spectroscopy investigation of light-induced degradation in p-type multicrystalline silicon PERC", *IEEE J. Photovolt.,* Vol. 6, No. 6, pp. 1466–1472, doi:10.1109/JPHOTOV.2016.2606699.
[14] Nakayashiki, K. et al. 2016, "Engineering solutions and root-cause analysis for light-induced degradation in p-type multicrystalline silicon PERC modules", *IEEE J. Photovolt.,* Vol. 6, No. 4, pp. 860–868, doi:10.1109/JPHOTOV.2016.2556981.
[15] Chen, D. et al. 2020, "Hydrogen-induced degradation: Explaining the mechanism behind light- and elevated temperature-induced degradation in n- and p-type silicon", *Sol. Energy Mater. Sol. Cells,* Vol. 207, p. 110353, doi:10.1016/j.

solmat.2019.110353.
[16] Wenham, A.C.N. et al. 2018, "Hydrogen-induced degradation", *Proc. 2018 IEEE 7th WCPEC*, Waikoloa, Hawaii, USA, pp. 1–8.
[17] Bredemeier, D. et al. 2019, "Impact of hydrogen-rich silicon nitride material properties on light-induced lifetime degradation in multicrystalline silicon", *physica status solidi (RRL)*, Vol. 13, No. 8, p. 1900201, doi:10.1002/pssr.201900201.
[18] Kersten, F., Heitmann, J. & Müller, J.W. 2016 "Influence of Al_2O_3 and SiN_x passivation layers on LeTID", *Energy Procedia*, Vol. 92, pp. 828–832, doi:10.1016/j.egypro.2016.07.079.
[19] Varshney U. et al. 2019, "Evaluating the impact of SiN_x thickness on lifetime degradation in silicon", *IEEE J. Photovolt.,* Vol. 9, No. 3, pp. 601–607, doi:10.1109/JPHOTOV.2019.2896671.
[20] Jensen, M.A. et al. 2018, "Evaluating root cause: The distinct roles of hydrogen and firing in activating light- and elevated temperature-induced degradation", *AIP J. Appl. Phys.,* No. 124, p. 85701, doi:10.1063/1.5041756.
[21] IEC 60891:2021 (Draft), "Photovoltaic devices – Procedures for temperature and irradiance corrections to measured I-V characteristics" (to be published in 2021).
[22] IEC TS 60904-1-2:2019, "Photovoltaic devices – Part 1-2: Measurement of current-voltage characteristics of bifacial photovoltaic (PV) devices".
[23] IEC 61853-1:2011, "Photovoltaic (PV) module performance testing and energy rating – Part 1: Irradiance and temperature performance measurements and power rating".
[24] IEC 60904-9:2020, "Photovoltaic devices – Part 9: Classification of solar simulator characteristics".
[25] Castro, J.B. et al. 2020, Climatic rating of photovoltaic modules: Different technologies for various operating conditions", Report IEA-PVPS T13-20:2020.
[26] Mavromatakis, F., Vignola, F. & Marion, B. 2017, "Low irradiance losses of photovoltaic modules", *Solar Energy*, Vol. 157, pp. 496–506.

About the Authors

Johanna Bonilla holds a B.Sc. in electrical engineering, with a two-year specialization in power systems. In early 2016 she received her master's in renewable energy from the University of Applied Sciences in Cologne, Germany, and then became a member of the solar team at TÜV Rheinland Energy. She joined JinkoSolar in 2020 as a technical service manager. Her expertise includes PV module characterization, PV modules and systems performance analysis, field failures and bifacial technologies.

Roman Giehl is responsible for technical business development in the DACH region and the Netherlands. Since 2003 he has been working for several leading PV manufacturers and distributors in the PV industry and joined JinkoSolar in 2016. Coming from a chemical engineering background, he has an in-depth knowledge of PV technology and module development, and expertise in polymers, metals, silicon and industry, which have enabled him to successfully support technical business development in Europe.

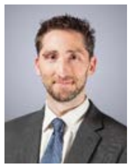

Calors Magistris has 17 years of work experience in the PV sector. Prior to joining JinkoSolar, he worked as an independent technical advisor and consultant, where he carried out various field-test services. He has also collaborated in the creation of the new IEC TS 62941 standard. Throughout his career, he has worked with developers, IPPs, EPCs, financial institutions and manufacturers in mitigating product and system risk in various markets. He is a member of the international PV committee IEC-TC82.

Roberto Murgioni holds a B.Sc. in electrical engineering and a master's in renewables and nuclear energy engineering. He joined JinkoSolar in 2017 and currently leads the Technical Service and Product Management team in the EU. He began working in PV in 2006 and has held a variety of similar positions at other Tier 1 module manufacturers. He has also worked as an expert project engineer for various EPC companies, managing large PV power plant projects in Europe, Latin America and Africa, including design, construction and commissioning.

Enquiries

Johanna Bonilla
JinkoSolar GmbH
Freisinger Str. 9
85716 Unterschleißheim bei München
Germany

Email: Johanna.bonilla@jinkosolar.com
Website: www.jinkosolar.eu